Quasigeoid Computation in Bavaria

C. Gerlach
Institute of Astronomical and Physical Geodesy,
Technische Universität München , Arcisstr. 21, D-80290 Munich, Germany

Abstract. A gravimetric quasigeoid has been computed for the area of Bavaria. The solution was derived using the theory of *analytical continuation*. The series expansion was carried out up to third order for both surface free-air and RTM-reduced gravity anomalies. A comparison shows the size and shape of the usually neglected higher order terms as well as the impact of topographic reductions. Data preprocessing involves coordinate transformation of all available gravimetric data to one single reference frame. Critical in this context is the height coordinate if datum offsets between different national height systems are not very well known. Such offsets are of the order of some decimeters in central Europe (with one extreme value of more than 2 meters for Belgium). Neglection of proper transformations leads to a tilt of the Bavarian geoid of the order of $1\,\mathrm{cm}/100\,\mathrm{km}$. The overall quality of the quasigeoid has been checked against height anomalies derived from GPS/levelling in Bavaria. After reduction of a second order trend function an RMS of 3cm was derived.

Keywords. quasigeoid, analytical continuation, height datum offsets, topographic reduction

1 Theoretical background

The determination of the physical surface of the earth from gravity anomalies is known as *Molodensky's problem*. Even though the surface anomalies are linear functions of the harmonic potential outside the masses they can not directly be used in Stokes integral because they refer to the physical surface which is not an equipotential surface of the gravity field. Application of Stokes' integral equation for geoid computation is still possible after some corrections have been applied to the free-air anomalies. In Molodensky's solution these are the so called *Molodensky correction* terms taking into account the inclination of the terrain. A different approach, called *analytical continuation*, was proposed by Moritz (see e.g. Moritz, 1980). Here all surface anomalies are analytically downward continued to the level surface passing through the computation point (or any other point level if desired). As they are analytically connected to the surface anomalies they represent the harmonic potential outside the earth even though they are situated inside the topographic masses. Therefore the requirements for application of Stokes theory are fulfilled and the height anomaly $\zeta(P)$ at computation point P can be computed according to

$$\zeta(P) \;=\; \frac{R}{4\pi\gamma}\iint\limits_{\sigma} \Delta g^*\, St(\psi)\, d\sigma, \qquad (1)$$

where Δg^* are the downward continued anomalies referring to the level surface through P, ψ is the spherical distance between computation and integration point and $St(\psi)$ is the Stokes function. According to Moritz (1980, sec. 45) the downward continued anomalies can be expanded into a series

$$\Delta g^* \;=\; g_0 + g_1 + g_2 + g_3 + \ldots \qquad (2)$$

each term being computable by the following recursion, starting from the surface anomalies Δg:

$$\begin{aligned} g_0 &= \Delta g \\ g_1 &= -\Delta h L_1(g_0) \\ g_2 &= -\Delta h L_1(g_1) - \Delta h^2 L_2(g_0) \\ g_3 &= -\Delta h L_1(g_2) - \Delta h^2 L_2(g_1) - \Delta h^3 L_3(g_0). \end{aligned} \qquad (3)$$

Here $\Delta h = h - h_P$ is the height difference between physical surface and level surface through P and the operator L_n can also be computed recursively by

$$L_n(f) \;=\; n^{-1} L_1(L_{n-1}(f)). \qquad (4)$$

The surface operator L_1 is given by

$$L_1(f) \;=\; \frac{R^2}{2\pi}\iint\limits_{\sigma} \frac{f - f_P}{l_0^3}\, d\sigma \;=\; \frac{\partial f}{\partial r}, \qquad (5)$$

where $l_0 \;=\; 2R\sin\frac{\psi}{2}$ is the distance between computation and integration point. Using these equations the height anomaly is computed by the series

$$\zeta \;=\; \zeta_0 + \zeta_1 + \zeta_2 + \zeta_3 + \ldots \qquad (6)$$

One can show (see e.g. Moritz, 1980, sec. 46) that this series is termwise equal to the solution using *Molodensky corrections*.

2 Computational methodology

As usually done in practical geoid determination a *remove – restore* procedure is applied. The gravity anomalies are reduced for some known or computable part of the signal whose effect on the geoid is added back after applying Stokes integral (1) on the reduced anomalies. This is done for the long wavelength part coming from a global potential model. In the present computations the Earth Gravity Model EGM96 was used. Gravity anomalies Δg^{EGM} and height anomalies ζ^{EGM} from EGM96 were processed according to the procedure given by Lemoine et al. (1998). The influence of the atmospheric masses is treated according to the IAG–approach, which is described e.g. in Moritz (1980, sec.49). The reduced anomaly reads

$$\Delta g_{red} \;=\; \Delta g - \Delta g^{EGM} + \delta g^{Atm}, \qquad (7)$$

where δg^{Atm} is the atmospheric gravity effect which can be taken from Moritz (1988). As the atmospheric effect on the height anomalies is usually quite small it is neglected in the *restore* procedure.

The reduced anomalies still refer to the earth surface but represent a reduced gravity field. They are still quite rough especially in mountainous areas (see figure 2) as EGM96 only removes the long and medium length structures of the field. In solving the geodetic boundary value problem for the physical surface of the earth no topographic reductions are necessary. Still topographic reductions smooth the gravity field and are therefore useful for both gridding purposes and a faster convergence of the series (6). As the potential model already includes the low frequency part of the topographic effect it seems most appropriate to use a *residual terrain model* (RTM) for reductions (see e.g. Forsberg and Tscherning, 1981). Using Bouguer or isostatic anomalies instead means to take into account topography twice. In the present case a $15' \times 15'$ reference topography was used, which corresponds to degree $n = 720$ of a spherical harmonic expansion and is well above the resolution of EGM96 with its $n_{max} = 360$. In practical geoid determination one usually assumes that the *Molodensky corrections* are very small when using RTM-reduced anomalies and often neglects them at all (see e.g. Torge and Denker, 1999; Grote, 1996). The validity of this assumption was shown by Denker and Tziavos (1999) by computing the *Molodensky corrections* for a test area in the Mont Blanc region of the European Alps. In this paper we will investigate the ζ_n terms using *analytical continuation* in a larger area.

The computations are carried out by fast spectral algorithms, i.e. by the 1D-FFT method proposed by Haagmans et al. (1993). The method can be applied to convolution integrals such as Stokes integral (1) or the downward continuation operator given in (5). For the Stokes integral we have

$$\zeta \;=\; \frac{R\Delta\varphi\Delta\lambda}{4\pi\gamma}\,\mathcal{F}_1^{-1}\Big\{\sum_{\varphi}\mathcal{F}_1\{\Delta g\cos\varphi\}\cdot\mathcal{F}_1\{St(\psi)\}\Big\} \qquad (8)$$

and for the L_1–operator

$$\begin{aligned} L_1(f) \;=\; \frac{R^2\Delta\varphi\Delta\lambda}{2\pi}\Big[&\mathcal{F}_1^{-1}\Big\{\sum_{\varphi}\mathcal{F}_1\{f\cos\varphi\}\cdot\mathcal{F}_1\{l_0^{-3}\}\Big\} \\ &- f\cdot\mathcal{F}_1^{-1}\Big\{\sum_{\varphi}\mathcal{F}_1\{\cos\varphi\}\cdot\mathcal{F}_1\{l_0^{-3}\}\Big\}\Big], \end{aligned} \qquad (9)$$

where $\mathcal{F}_1\{\cdot\}$ denotes 1D–Fourier transformation and $\mathcal{F}_1^{-1}\{\cdot\}$ denotes the inverse transformation.

3 Data and preprocessing

3.1 Gravimetric data

Point and block mean gravity values were collected in a $4°$-cap around Bavaria. In a preprocessing step all values were transformed, first, to one single reference frame and, secondly, to a consistent set of equally sized block mean values by least squares prediction. The horizontal position of the points was transformed to ETRS89. The height component was shifted to the German system DHHN92, which is close to the United European Leveling Network UELN95 (offset 1 cm, see (Sacher et al., 1999)). Transformation does not only affect the coordinates but due to $\gamma = \gamma(h, \varphi)$ also the values of the gravity anomalies, where the height component is the most critical part. Sacher et al. (1999) have reported transformation relations between national height systems

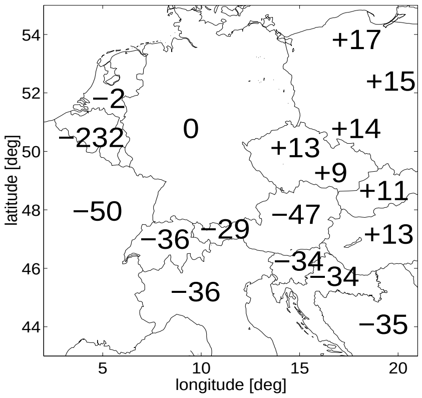

Fig. 1. Differences between DHHN92 normal heights and national height systems in cm. Difference between UELN95 and DHHN92 is +1cm. [taken from: Sacher et al. (1999)]

and the UELN95 (see Figure 1). Those were used for the present computations. The height differences include not only offsets due to different datum points but also the effect of different types of height like normal or orthometric height.

3.2 Topographic data

Height information is necessary both for topographic reductions as well as for computing the g_n terms according to (3). In the present computation Digital Height Models (DHM) of different resolution have been used, from 30" $\times$ 30" down to $50\text{m}\times 50\text{m}$ in Bavaria. The reductions are based on simple prism bodies. The resolution of the reference topography was $15' \times 15'$. For computation of the g_n terms the 30" $\times$ 30" DHM was used in the entire area. The results of Denker and Tziavos (1999) show that the evaluated height anomaly differs only by some few centimeters in rough terrain if a 30" $\times$ 45" DHM is used instead of a dense 7.5" $\times$ 7.5" DHM. This corresponds to the results obtained by Grote (1996). For smoother terrain the difference is even less. Figure 2 shows the effect of RTM reduction on surface free air anomalies. As stated earlier the reduced anomalies still refer to the real earth surface but represent a smoothed topography. They can be seen as analytically continued values from the smoothed to the real surface. It is worthwhile noticing the strong correlation between Δg_{FA} and height in case of rough terrain. In lowlands there is no such correlation. Mind that in figure 2 the EGM effect is already substracted so that there is only a small signal left in lowlands.

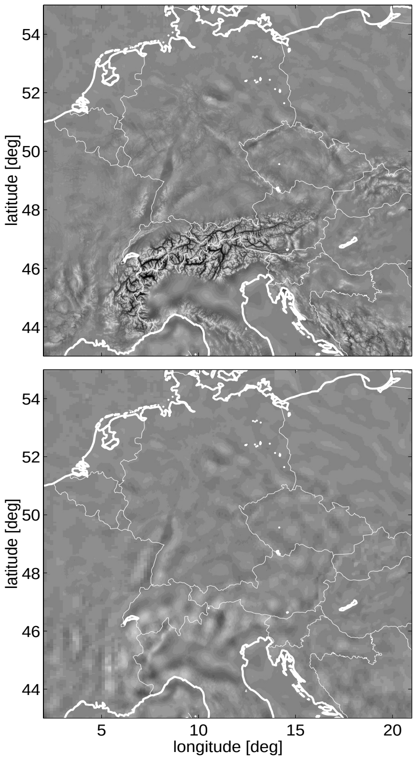

Fig. 2. Surface free-air anomalies Δg_{FA} (top) and RTM-reduced anomalies Δg_{RTM} (bottom). Both are reduced for the global effect of EGM96. The anomalies reach values up to ± 250 mGal in case of Δg_{FA} and ± 80 mGal for Δg_{RTM}.

4 Numerical investigations

4.1 Effect of height system offsets on the geoid

Lacking information about the reference frame of some given data and the connection to the chosen computation reference frame one must forego transformations in the preprocessing step. This often happens in practice, when one is collecting data from different institutions. Therefore it is interesting to see, how such unknown offsets between different national heights affect the geoid. Two geoid computations were carried out, one based on the original (not transformed) heights and another one including transformation to DHHN92 according to the numbers given in figure 1. Comparison shows for the Bavarian geoid a tilt of $0.7\,\text{cm}/100\,\text{km}$ in north–eastern direction. The effect is shown in Figure 3.

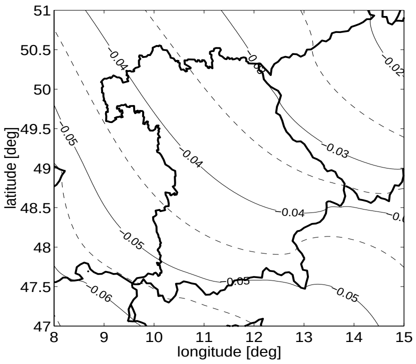

Fig. 3. Bias of Bavarian geoid induced by datum offsets between different national height systems.

4.2 Effect of RTM reductions on the geoid

One usually assumes that smoothing the gravity field by RTM reductions reduces the size of the Molodensky correction term. Series (6) should converge faster in that case. This can be seen from the following representation in spherical harmonics. The gravity anomaly is given by

$$\Delta g \;=\; \sum_{n=2}^{\infty} \left(\frac{R}{r}\right)^{n+2} \Delta g_n(\theta,\lambda), \qquad (10)$$

where $g_n(\theta,\lambda)$ are the surface spherical harmonics. Then the gradient $\partial/\partial r$ is given by

$$\frac{\partial \Delta g}{\partial r} \;=\; -\sum_{n=2}^{\infty} \left(\frac{R}{r}\right)^{n+2} \frac{n+2}{r} \Delta g_n(\theta,\lambda) \quad (11)$$

and so for $r = R$ we get

$$\left(\frac{\partial \Delta g}{\partial r}\right)_n \;=\; -\frac{n+2}{R}\,\Delta g_n. \qquad (12)$$

If we restrict ourselves to a first order expansion (1) reads, using equations (2) and (3),

$$\zeta(P) \;=\; \frac{R}{4\pi\gamma} \iint_\sigma \left(\Delta g - \frac{\partial \Delta g}{\partial r}\Delta h\right) St(\psi)\, d\sigma. \qquad (13)$$

According to equation (12) the anomaly gradient is much smaller than the anomaly itself because of the factor $1/R$. Only the high frequencies can gain considerable size where the factor $(n+2)$ counteracts $1/R$. That means the second term in (13) must be taken into account depending on the size of the high frequency part in the anomaly signal. If there is only small power in the high frequencies it can be neglected. This is the case when the field is smoothed by topographic reductions. Figures 4 and 5 show the results of the computations carried out using the unsmoothed free-air anomalies and the smoothed RTM-anomalies. Of course the largest signal shows up in the Alps because the gravity anomalies reach their highest values there. Stokes' integration smoothes the high frequency gravity signal and spreads it over a larger area. This results in a tilt for areas outside the Alps region. Comparison of the first order term ζ_1^{FA} shows that for free-air anomalies (FA) the contribution to the height anomaly is quite large and reaches the same order of magnitude as the zero order terms ζ_0^{FA} and ζ_0^{RTM}. Its high positve values counteract the negative signal coming from ζ_0^{FA}. In comparison, ζ_1^{RTM} amounts to one decimeter values only, which is less more than one order of magnitude. The terms ζ_2^{RTM} and ζ_3^{RTM} decrease quite fast by a factor of $1/10$ per order. Using free-air anomalies the convergence of the series is much slower. ζ_2^{FA} and ζ_3^{FA} still reach values up to one decimeter. Again ζ_3^{FA} counteracts ζ_2^{FA}, which gives the free-air series an alternating character (it is not really alternating, because the first and second order terms have the same sign).

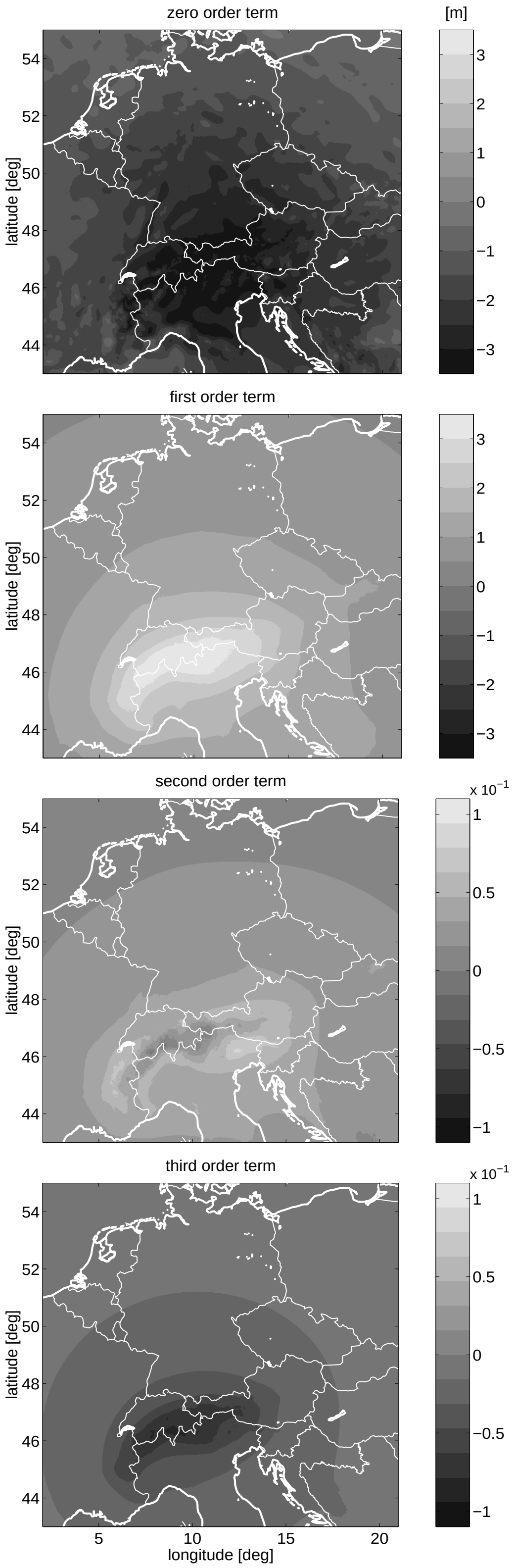

Fig. 4. Height anomaly from free-air gravity anomalies

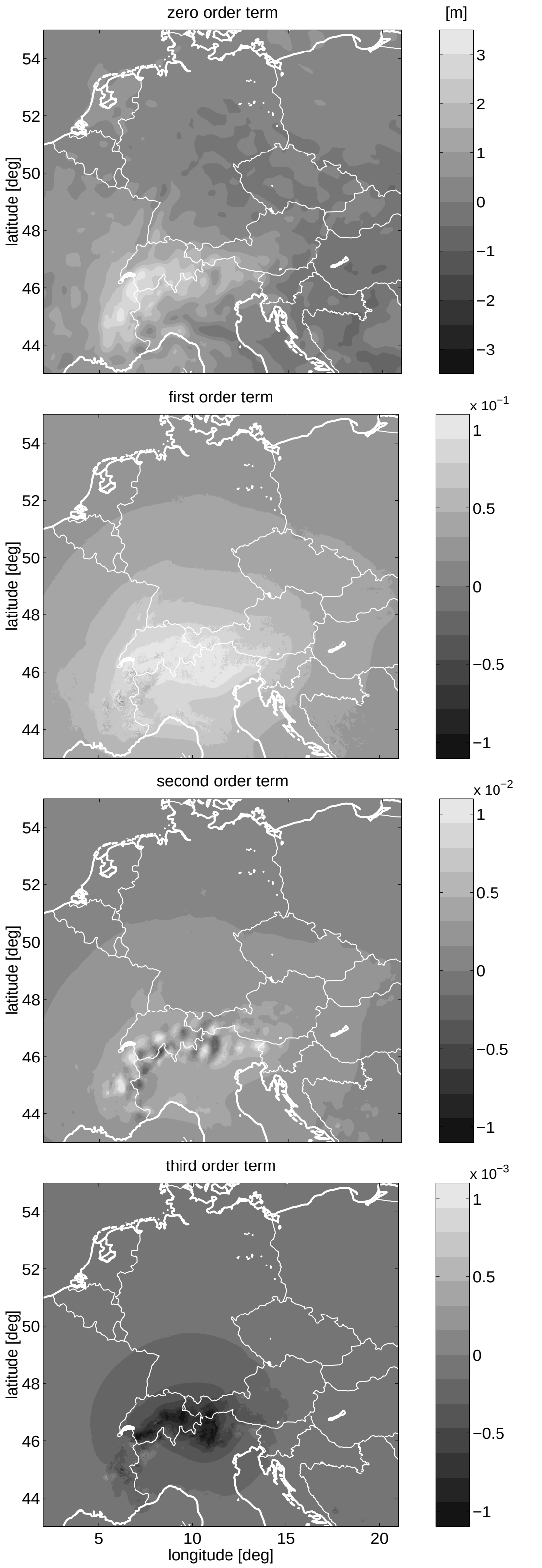

Fig. 5. Height anomaly from RTM-reduced gravity anomalies

4.3 Comparison to height anomalies from GPS/levelling

To get an idea of the overall accuracy obtained by the above computations the quasigeoid was compared to height anomalies derived by GPS/levelling in Bavaria. A set of 97 control points with an estimated accuracy of $2-3$ cm was used. The differences (see figure 6, top) show a significant tilt of about $10\,\mathrm{cm}/100\,\mathrm{km}$ in south–eastern direction. This order of magnitude fits to the findings of other quasigeoid computations, like e.g. EGG97. Torge and Denker (1999) report tilts of around 1.5 ppm for the same region. The reason for such a bias is not fully understood until now, but propagation of EGM errors is a strong candidate. A low order correction surface can be used to fit the gravimetric solution to the GPS/levelling results. A second order surface was used for the present computations. The residuals given in figure 6 (bottom) show minima and maxima at -9.8 cm and 8.2 cm with an RMS of 3 cm. These numbers are derived from the solution obtained from the RTM-reduced anomalies. Using the free-air anomalies the same accuracy is achieved after trend reduction.

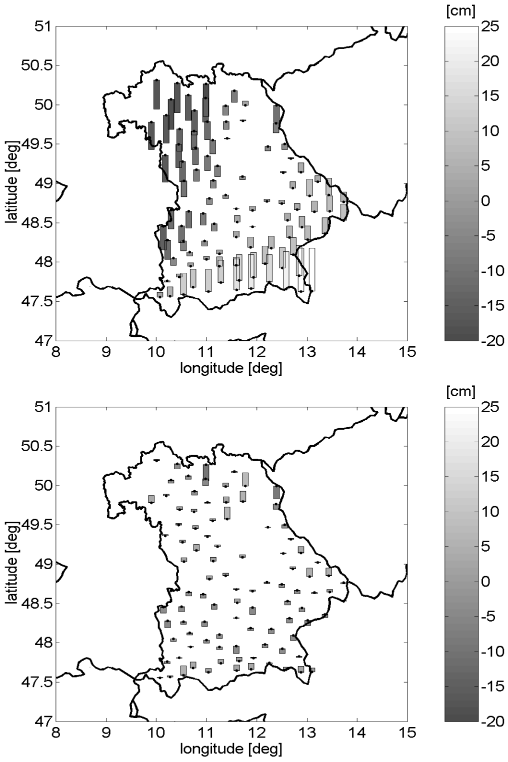

Fig. 6. Raw (top) and trend reduced (bottom) differences between the gravimetric quasigeoid and height anomalies derived from GPS/levelling at 97 points in Bavaria.

5 Discussion

It is shown that smoothing the gravity field by topographic reductions is very favourable to the convergence of the series solution for the height anomaly. The first order term gives a contribution of up to one decimeter in the Alps and a slight tilt in the surrounding areas. Aiming at centimeter accuracy the second order term is only significant in very rough topography, giving maximum contributions of 1 cm, while the third order term can be neglected in any region. For a solution derived from unreduced free-air anomalies the series converges much slower and even the third order term shows values up to one decimeter in the Alps.

The whole solution is biased compared to height anomalies derived from GPS/levelling, assumedly due to propagation of EGM errors. The gravimetric solution is fitted to the GPS/levelling height anomalies using a low order correction surface. In Bavaria such a low order surface takes care not only of the EGM errors but also of the tilt caused by the first order term as well as for the bias introduced by disregarding the proper transformation of all gravimetric data to one height system. This leads to the conclusion that one can restrict the gravimetric solution to the zero order term and might neglect datum offsets in preprocessing, if in a postprocessing step a low order correction surface is considered acceptable to fit the solution to GPS/levelling points. This is not valid for areas in the central region of the Alps where the contribution of the higher order terms is not so smooth.

Choosing for the correction surface a second order function seems to be appropriate in Bavaria because the trend is not a mere plane, but the inclination is steeper close to the Alps. Of course higher order correction surfaces give a better fit to GPS/levelling. But one should be aware that fitting to GPS/levelling tends to bend the gravimetric solution, which is assumed to represent short wavelengths with highest accuracy. Some arbitrariness is introduced this way. Further investigations are needed for a theoretical formulation of the problem.

References

Denker H, Tziavos IN (1999) Investigation of the Molodensky series terms for terrain reduced gravity field data. Bolletino di Geofisica Teorica ed Applicata, vol. 40, no. 3–4 pp. 195–203.

Forsberg R, Tscherning CC (1981) The Use of Height Data in Gravity Field Approximation by Collocation. Journal of Geophysical Research, vol. 86, no. B9, pp 7843–7854.

Grote T (1996) Regionale Quasigeoidmodellierung aus heterogenen Daten mit cm-Genauigkeit. Wissenschaftliche Arbeiten der Fachrichtung Vermessungswesen der Universität Hannover, no. 212.

Haagmans R, de Min E, van Gelderen M (1993) Fast evaluation of convolution integrals on the sphere using 1D FFT, and a comparison with existing methods for Stokes' integral. manuscripta geodatica no.18, pp. 227–241, Springer-Verlag.

Lemoine FG et al. (1998) The Develpoment of the Joint NASA GSFC and the National Imagery and Mapping Agency (NIMA) Geopotential Model EGM96. NASA Technical Publication NASA/TP–1998–206861, Goddard Space Flight Center, Greenbelt, MD.

Moritz H (1980) Advanced Physical Geodesy. H.Wichmann Verlag, Karlsruhe.

Moritz H (1988) Geodetic Reference System 1980. bulletin geodesique, vol. 62, no. 3, pp. 388–398.

Sacher M, Ihde J, Seeger H (1999) Preliminary Transformation Relations between National European Height Systems and the United European Levelling Network (UELN). In: Gubler, Torres and Hornik (eds.) Report on the Symposium of the IAG Subcommission for Europe (EUREF) held in Prague, 2–5 June 1999. Veröffentlichungen der Bayerischen Kommission für die Internationale Erdmessung, no. 60, München.

Torge W, Denker H (1999) Zur Verwendung des Europäischen Gravimetrischen Quasigeoids EGG97 in Deutschland. Zeitschrift für Vermessungswesen, no. 5/1999, pp. 154–166.